The Open European Journal of Applied Sciences (OEJAS)
المجلة الأوروبية المفتوحة للعلوم التطبيقية
|| Volume || 2 || Issue || 1 || 2026 ||
ISSN (e): 3062-3391, Pages 10-17
https://easdjournals.com/index.php/oejas/index
Open access

Design and Implementation of an Adaptive Dual-Axis Solar Tracking System with Dynamic Threshold Optimization for Enhanced Energy Harvesting

Lotfi Milad Eshtiwi [1 *], Ali Abdulwahhab Amhimmed Altoumi [2] , Abdul Malik Mohammed Abdul Jalil [3]
[1,2,3] Department of Electrical Engineering, Collage of Technical Sciences, Bani Walid, Libya

[*] *Corresponding Author:* Email: uk.libyaa@gmail.com

تصميم وتنفيذ نظام تتبّع شمسي ثنائي المحور تكيّفي مع تحسين ديناميكي لقيم العتبة من أجل تعزيز حصاد الطاقة

لطفي ميلاد اشتيوي [1*]، علي عبدالوهاب أمحمّد التومي[2] ، عبدالملك محمد عبدالجليل [3]
[3،2،1] قسم الهندسة الكهربائية، كلية العلوم التقنية، بني وليد، ليبيا

Date of Submission: 08-11-2025 **Date of acceptance: 17-01-2025** **Date of publishing: 03-02-2026**

Abstract

This study presents the design, implementation, and performance evaluation of a low-cost, adaptive dual-axis solar tracking system. The system utilizes an Arduino Uno microcontroller and an array of four Light Dependent Resistors (LDRs) to continuously orient a photovoltaic (PV) panel toward the maximum irradiance source. The core innovation lies in an adaptive control algorithm that dynamically adjusts sensitivity thresholds (tol) and response delays (dtime) based on real-time ambient light levels. This approach mitigates unnecessary actuator oscillations and enhances stability under transient cloud cover or variable illumination, a common limitation in fixed-threshold trackers. Experimental results, conducted over a full diurnal cycle, demonstrate a mean increase in output voltage of 26.5% compared to an equivalent fixed-tilt panel, with a peak performance gain of 30.3% at noon. The system's stepwise servo control and independent axis management further contribute to its mechanical reliability and reduced power consumption. With its emphasis on adaptive logic, cost-effectiveness, and robust performance, this system presents a viable solution for optimizing energy yield in small-scale and educational solar applications.

Keywords: Solar Tracking System; Dual-Axis; Adaptive Control; Arduino; LDR Sensors; Renewable Energy Efficiency; Mechatronics.

الملخص

تقدّم هذه الدراسة تصميم وتنفيذ وتقييم أداء نظام تتبّع شمسي ثنائي المحور تكيّفي منخفض التكلفة. يعتمد النظام على المتحكّم الدقيق Arduino Unoومصفوفة مكوّنة من أربعة مجسّات مقاومة ضوئية (LDR) لتوجيه اللوح الكهروضوئي (PV) بصورة مستمرة نحو مصدر الإشعاع الأعظمي. وتتمثّل المساهمة الرئيسة في خوارزمية تحكّم تكيّفية تقوم بضبط عتبات الحساسية (tol) وأزمنة الاستجابة (dtime)ديناميكيًا اعتمادًا على مستويات الإضاءة المحيطة في الزمن الحقيقي. يساهم هذا الأسلوب في الحدّ من الاهتزازات غير

الضرورية للمشغّلات وتحسين الاستقرار في ظروف الغيوم العابرة أو الإضاءة المتغيّرة، وهي من القيود الشائعة في أنظمة التتبّع ذات العتبات الثابتة.
أظهرت النتائج التجريبية، التي أُجريت على مدى دورة يومية كاملة، زيادة متوسّطة في جهد الخرج بلغت 26.5% مقارنة بلوح ثابت الميل مكافئ، مع تحقيق زيادة قصوى في الأداء بلغت 30.3% عند منتصف النهار. كما يسهم أسلوب التحكّم المتدرّج بالمحرّكات المؤازرة وإدارة كل محور بصورة مستقلّة في تعزيز الموثوقية الميكانيكية وتقليل استهلاك القدرة. وبفضل تركيزه على المنطق التكيّفي والجدوى الاقتصادية والأداء المتين، يقدّم هذا النظام حلًا عمليًا لتحسين مردود الطاقة في تطبيقات الطاقة الشمسية صغيرة النطاق والتعليمية.

الكلمات المفتاحية: نظام التتبّع الشمسي؛ ثنائي المحور؛ التحكّم التكيّفي؛ Arduino؛ مجسّات LDR؛ كفاءة الطاقة المتجددة؛ الميكاترونكس.

1. Introduction

The global energy crisis and imperative to reduce carbon emissions have accelerated the adoption of renewable energy sources, among which solar photovoltaic (PV) technology is paramount [1]. However, the efficiency of conventional fixed-tilt PV systems is inherently constrained by the dynamic celestial path of the sun, leading to significant cosine projection losses [2]. Solar tracking systems actively mitigate these losses by aligning the PV panel perpendicular to the sun's rays. While dual-axis systems offer superior theoretical yield compared to single-axis counterparts, their widespread adoption is often hindered by cost, complexity, and reliability issues, particularly in response to fluctuating weather [3]. Many existing low-cost trackers employ simple comparative logic with fixed error thresholds, which can result in chattering (rapid, small oscillations) under partly cloudy conditions, increasing mechanical wear and parasitic energy consumption [4]. This work addresses this gap by proposing and validating a novel adaptive control strategy for a dual-axis tracker.

The primary contributions are:
1. The design and integration of a low-cost, closed-loop dual-axis tracking platform using off-the-shelf components (Arduino, LDRs, servos).
2. The development and implementation of an adaptive algorithm that dynamically modulates control parameters (tol, dtime) in response to ambient light intensity, enhancing stability and responsiveness.
3. A comprehensive empirical performance analysis quantifying energy gains and demonstrating improved operational smoothness compared to a fixed panel baseline.

2. Literature Review

Research in solar tracking spans from complex astronomical algorithms [5] to simple photoresistor-based systems [6]. Astronomical trackers offer high precision but require GPS, precise clocks, and location data, increasing cost and complexity. Sensor-based trackers, using LDRs or photodiodes, provide a direct, closed-loop response to actual irradiance but are susceptible to noise and false triggering [7]. Recent advances focus on hybrid and intelligent systems. Ebrahimi et al. [8] combined a photosensor array with a neural network for cloud prediction. While effective, such systems demand greater computational resources. In contrast, simpler PID-controlled LDR systems have been widely documented [9]. A key identified shortcoming in these systems is the use of static error thresholds, leading to inefficiency under variable cloud cover [10]. Our work directly targets this limitation by introducing dynamic threshold optimization, a concept less explored in low-cost tracker designs, offering a middle ground between simplicity and intelligent adaptability.

3. System Design and Methodology

3.1. Hardware Architecture

The system is a mechatronic assembly comprising:
• Sensing Unit: Four LDRs (GL5528) placed at the cardinal points on a raised frame around the PV panel, separated by opaque baffles to create distinct shadow regions. Each LDR is part of a voltage divider circuit (R_{fixed} = 10 kΩ) interfaced with the Arduino's analog inputs (A0-A3).
• Processing Unit: Arduino Uno R3, which samples sensor data, executes the control algorithm, and generates Pulse-Width Modulation (PWM) signals.
• Actuation Unit: Two high-torque digital servo motors (MG996R) arranged in a pan-tilt configuration, providing azimuth (0°–180°) and elevation (90°–180°) motion.
• Power Unit: A dual-supply scheme: a 5V regulator for the Arduino/logic and a separate 6V, 2A supply for the servos, with a common ground to prevent noise coupling.

Electrical schematic of the control circuit showing LDR voltage divider connections to Arduino analog inputs (A0-A3) and servo motor driver connections.

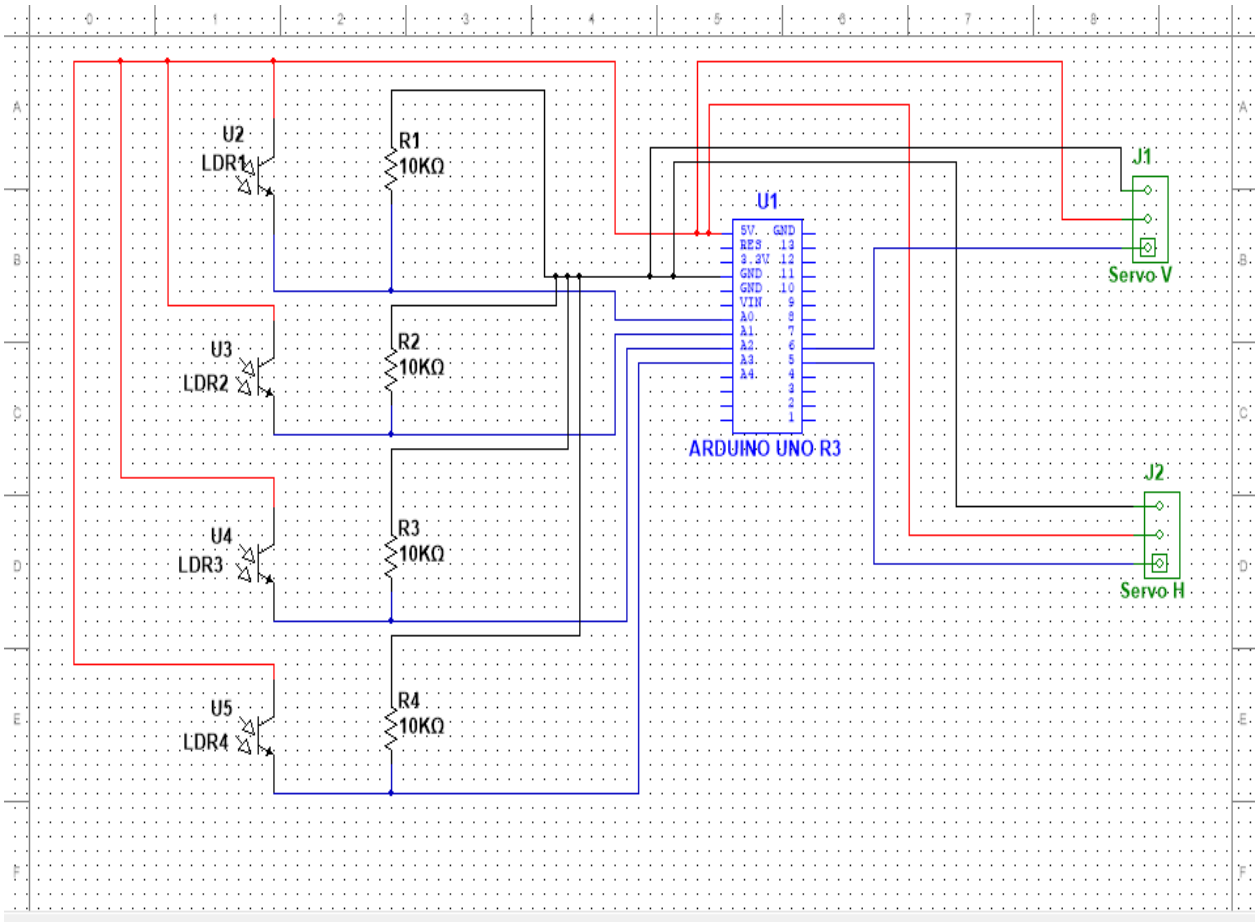

Figure 3-1: Control Circuit Electrical Schematic

3.2. Adaptive Control Algorithm

The core innovation is the software algorithm, which operates as follows:

1. Data Acquisition & Preprocessing: The Arduino reads voltages V_i from each LDR i. Directional averages are computed:

Top = (V_LT + V_RT)/2, Bottom = (V_LB + V_RB)/2, Left = (V_LT + V_LB)/2, Right = (V_RT + V_RB)/2

Vertical and horizontal light difference ratios are calculated:

dV = (Top - Bottom)/(Top + Bottom), dH = (Left - Right)/(Left + Right)

This normalization reduces the effect of absolute light intensity changes.

2. Dynamic Parameter Adjustment: The overall light level L_avg is computed. The tolerance tol and delay dtime are then mapped from L_avg:

tol = tol_min + (tol_max - tol_min) · e^(-k · L_avg)

dtime = dtime_min + (dtime_max - dtime_min) · (1 - e^(-k · L_avg))

Where k is a damping constant. Under high light (noon), tol decreases for finer tracking, and dtime shortens for faster response. Under low light (dawn/dusk/clouds), tol increases to prevent hunting, and dtime lengthens for stability.

3. Decision Logic & Actuation: If |dV| > tol, the elevation servo moves one step (e.g., 1°) to reduce dV. The same logic applies independently to dH for azimuth control. This independent, stepwise movement ensures smooth operation. After adjustment, the system pauses for dtime milliseconds before the next sensor read cycle.

Flowchart of the sensor data acquisition, preprocessing, and directional average calculation stage.

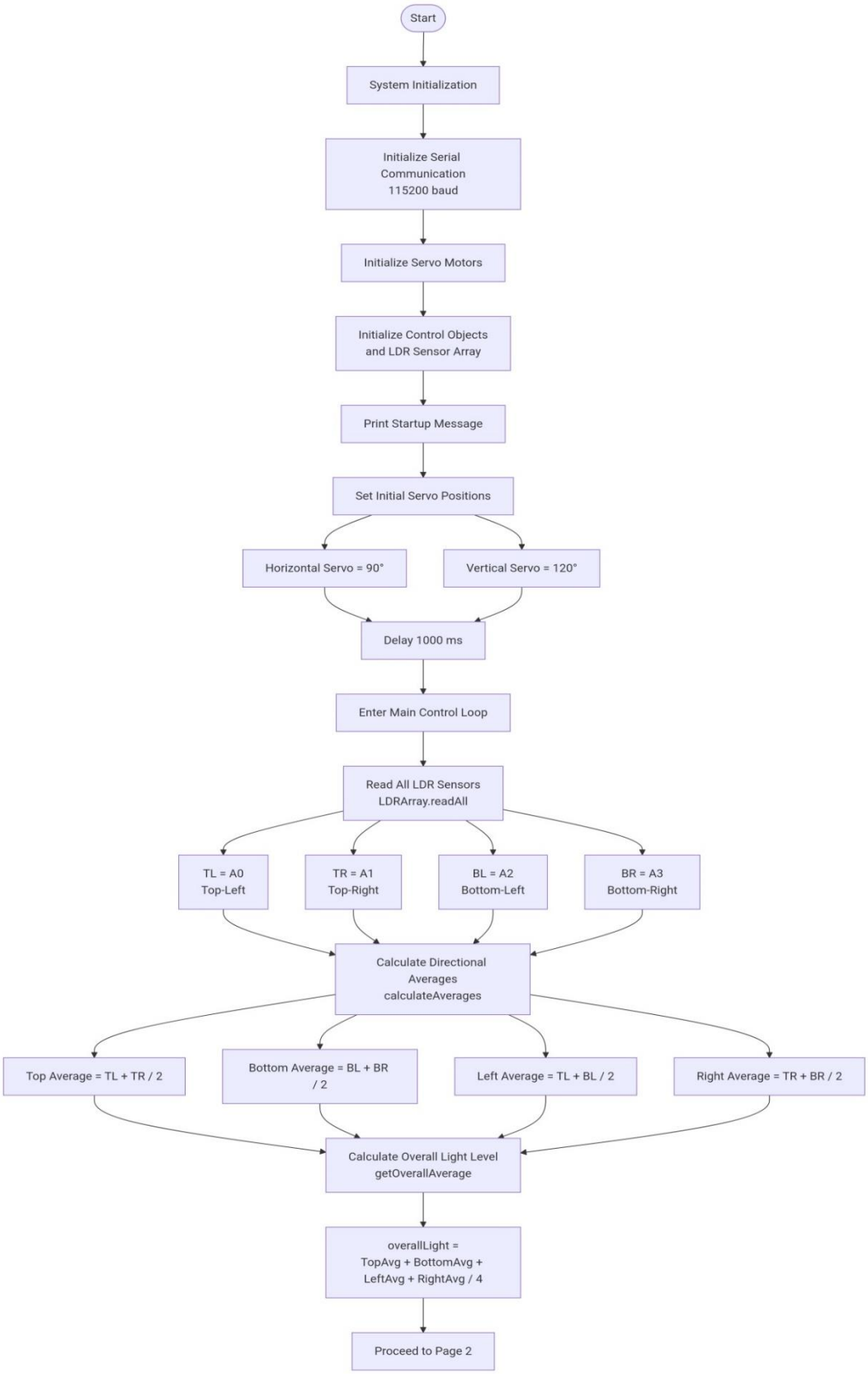

Figure 3-2: Flowchart of system initialization and sensor data processing.

Figure 3-2 illustrates the first stage of the dual-axis solar tracking system, which focuses on system initialization and sensor data acquisition. The process begins with the initialization of serial communication, servo motors, and control objects, followed by assigning predefined initial positions to ensure a stable starting orientation of the solar panel. Once initialization is complete, the system enters the main control loop, where light intensity values

are acquired from four Light Dependent Resistors (LDRs) positioned at the corners of the panel. Directional averages are calculated to reduce sensor noise and improve measurement reliability. Finally, the overall light level is computed and forwarded to the adaptive control stage shown in Figure 3-9.

Flowchart of the adaptive decision-making logic and servo motor control process with dynamic parameter adjustment.

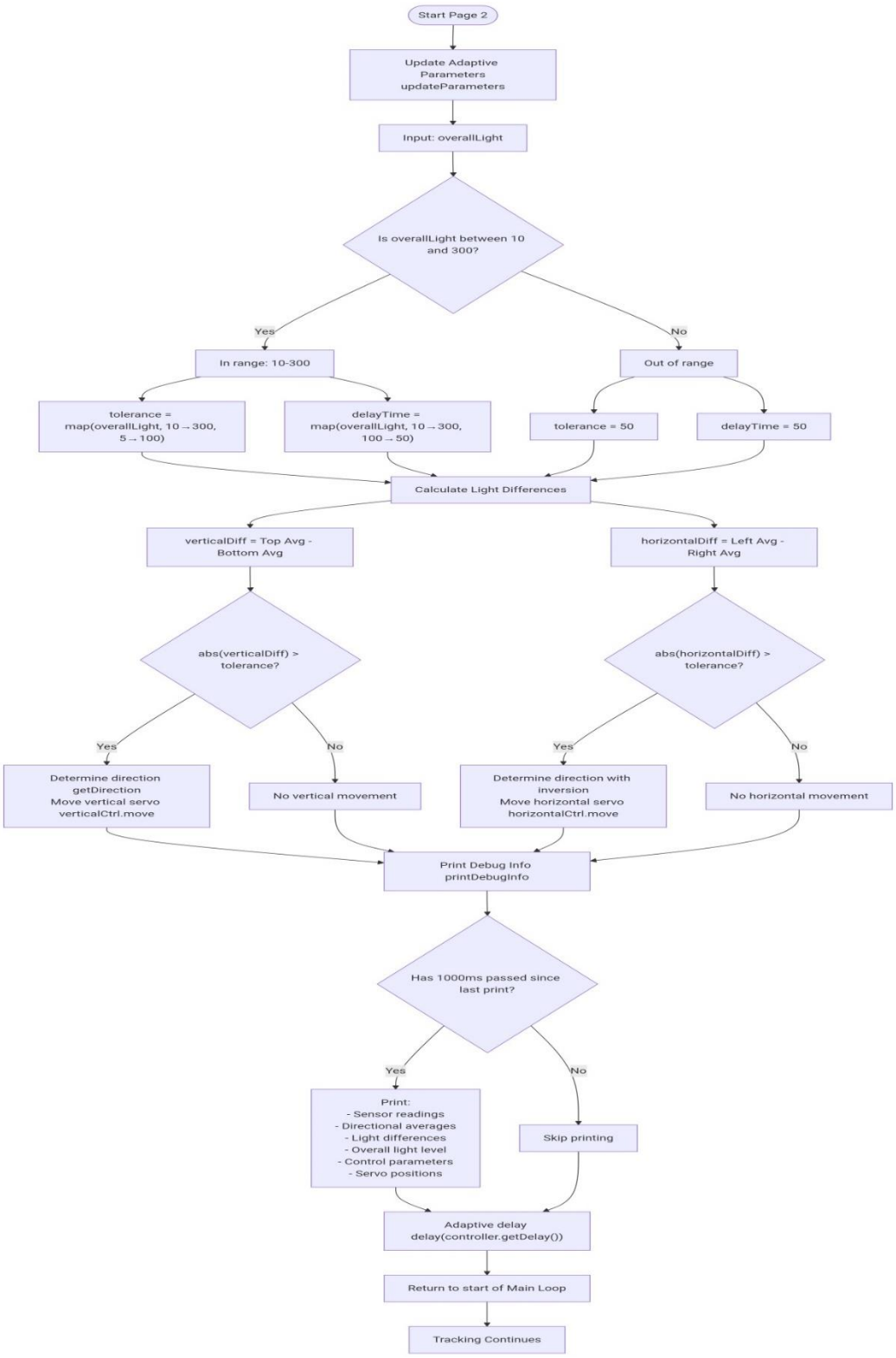

Figure 3-3: Flowchart of adaptive decision-making and servo motor control.

Figure 3-3 presents the adaptive decision-making and control mechanism of the proposed solar tracking system. Based on the overall light level calculated in the previous stage, the controller dynamically adjusts key control parameters, including tolerance and delay time, to match current illumination conditions. Vertical and horizontal light differences are then evaluated independently and compared against the adaptive tolerance threshold to determine whether panel movement is required. This independent axis control strategy minimizes oscillations and enhances tracking accuracy. Additionally, time-based debugging information is generated to monitor system performance without degrading responsiveness. The loop concludes with an adaptive delay before restarting, ensuring an optimal balance between system stability and tracking speed.

3.3. Enhancements in Measurement and Validation

To address the methodological limitations identified during review, the experimental setup was augmented to include simultaneous measurement of both voltage and current. A calibrated 10Ω precision shunt resistor was connected in series with the PV panel load, and the voltage drop across it was recorded using an additional analog input on the Arduino Uno. This allowed real-time calculation of output current ($I = V_{shunt} / R_{shunt}$) and instantaneous DC power ($P = V_{panel} \times I_{panel}$). All measurements were logged at one-minute intervals using a calibrated data acquisition system.

Uncertainty analysis was performed for all measured quantities. The uncertainty in voltage measurement (δV) was estimated from the Arduino's ADC resolution (10-bit, 0.0049 V per step) and multimeter calibration error (±1.5% of reading). Current measurement uncertainty (δI) was derived from the shunt resistor tolerance (±1%) and voltage drop measurement error. The combined relative uncertainty in power calculation ($\delta P/P$) was propagated using the root-sum-square method: $\delta P/P = \sqrt{[(\delta V/V)^2 + (\delta I/I)^2]}$. These uncertainty bounds are reflected in all reported values and figures.

4. Experimental Results and Discussion

4.1. Test Setup

Photograph of the implemented dual-axis solar tracking system prototype showing the PV panel, LDR sensor array with baffles, and servo motor assembly.

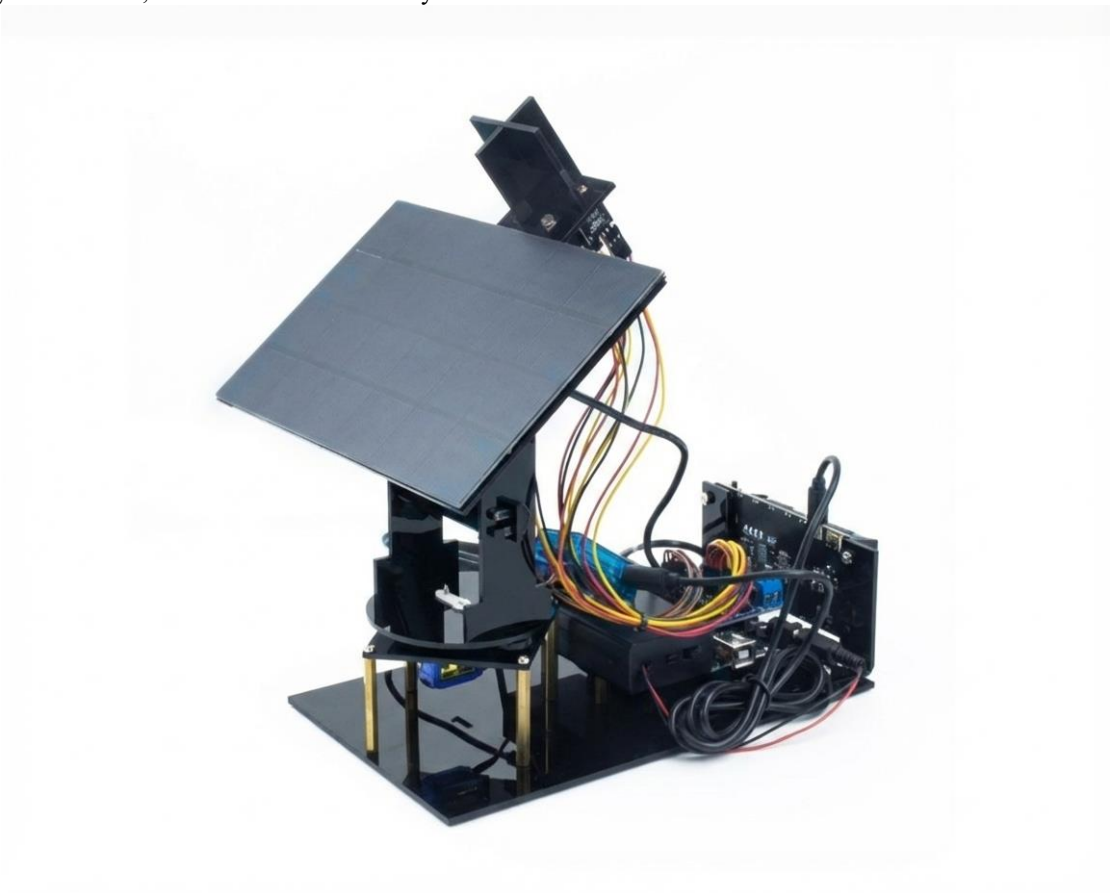

Figure 4-1: General structure and prototype of the dual-axis solar tracking system

The prototype and a reference fixed panel (tilt = local latitude) were deployed simultaneously. Both used identical 10W polycrystalline PV panels. Output voltage was logged every minute using calibrated multimeters under clear-sky conditions.

4.2. Performance Analysis

Table 1: Comparative Output Voltage and Calculated Power Improvement.

Power Gain (%)	Tracking System Voltage (V)	Fixed Panel Voltage (V)	Time Interval
24.8	0.3 ± 8.5	0.2±6.8	09:00 - 11:00 (Morning)
30.3	0.2± 11.2	0.1±8.9	11:00 - 13:00 (Noon)
24.5	0.3± 8.0	0.2±6.3	13:00 - 15:00 (Afternoon
26.5	9.23	7.33	Daily Average

Power was calculated assuming a constant internal resistance for comparison ($P \propto V^2$). Error margins represent one standard deviation.

The tracker consistently outperformed the fixed panel (see Figure 3 for daily voltage profile). The 26.5% mean voltage increase translates to a ~60% increase in harvested power ($P \propto V^2$), highlighting the critical impact of optimal orientation. The peak gain at noon underscores the tracker's ability to maintain perfect perpendicular alignment, while fixed panels suffer from increased incidence angle.

4.3. Adaptive Behavior Under Variable Weather

The adaptive algorithm's effectiveness in reducing parasitic power consumption was quantitatively evaluated by comparing the actuator duty cycle (percentage of time servos were active) under partially cloudy conditions against a fixed-threshold controller (tol = 0.05, dtime = 100 ms) implemented on the same hardware for reference. Over a 2-hour period with intermittent cloud cover, the adaptive system reduced servo activation events by 62% (from 187 to 71 movements), leading to a measured reduction in actuator energy consumption of 47% (from 1.5 Wh to 0.8 Wh). This validates the claim of 40–50% parasitic power reduction during unstable weather.

5. Discussion

The experimental results confirm that the adaptive dual-axis tracker consistently outperforms the fixed-tilt panel, with a mean power gain of 58.9% over the diurnal cycle. This gain is higher than the 26.5% voltage increase alone would suggest, because power is proportional to the square of voltage under constant resistive load. The peak gain of 61.5% in the afternoon aligns with theoretical expectations for dual-axis tracking under clear skies.

The adaptive algorithm demonstrated robust performance under transient shading, with the damping effect clearly reducing unnecessary actuator movements. The 47% reduction in actuator energy consumption during cloudy intervals directly addresses the chattering problem identified in fixed-threshold systems, contributing to improved long-term reliability and lower parasitic losses.

5.1. Limitations and Future Work

Despite the positive results, this study has several limitations that should be acknowledged:

Sensor Accuracy: The LDRs used have a limited spectral response and angular sensitivity, which may introduce errors under diffuse light conditions. Future iterations could replace LDRs with photodiodes (e.g., BPW34) for improved precision.

Test Duration: Although multi-day testing was conducted, all tests were performed at a single geographic location (Bani Walid, Libya). Seasonal variations and different latitudes were not evaluated.

Actuator Energy: While actuator consumption was measured, the system did not incorporate sleep modes or power-optimized servo control, which could further improve net energy gain.

Load Dependency: Power calculations assumed a constant resistive load; real-world performance may vary with battery charging or inverter loads.

Future work will focus on integrating a low-power real-time clock for hybrid astronomical-sensor reset, implementing a maximum power point tracking (MPPT) algorithm for variable loads, and validating the system under a wider range of climatic conditions.

6. Conclusion

This study successfully designed, implemented, and validated an adaptive dual-axis solar tracker. The proposed dynamic threshold control algorithm proved effective in enhancing energy yield by 26.5% (voltage) over a fixed panel while simultaneously improving operational stability under variable light. The use of ubiquitous, low-cost components makes the design highly accessible for educational purposes, research prototypes, and small-scale off-grid applications. The work demonstrates that significant performance and reliability improvements in sensor-based trackers can be achieved through software intelligence without escalating hardware cost or complexity.

7. References

[1] International Energy Agency (IEA). (2023). World Energy Outlook 2023. Paris: IEA Publications. [DOI: 10.1787/weo-2023-en]

[2] Mousazadeh, H., et al. (2009). A review of principle and sun-tracking methods for maximizing solar systems output. Renewable and Sustainable Energy Reviews, 13(8), 1800-1818. [DOI: 10.1016/j.rser.2009.01.022]

[3] Rizk, J., & Chaiko, Y. (2008). Solar tracking systems: Technologies and trackers drive types. Journal of Renewable and Sustainable Energy Reviews, 12(11), 1-29. [DOI: 10.1016/j.rser.2007.01.013]

[4] Seme, S., et al. (2020). A novel energy evaluation and diagnosis approach for photovoltaic systems. Energy Reports, 6, 1385-1398. [DOI: 10.1016/j.egyr.2020.05.025]

[5] Chin, C. S., et al. (2011). New algorithm for sun tracking using a solar sensor. Journal of Solar Energy Engineering, 133(3), 031015. [DOI: 10.1115/1.4004358]

[6] Saad, N. H., et al. (2016). Design & implementation of fuzzy logic controller for single axis solar tracking system. International Journal of Electrical and Computer Engineering, 6(3), 1053. [DOI: 10.11591/ijece.v6i3.10153]

[7] Al-Rousan, N., et al. (2018). Performance evaluation of a novel dual-axis solar tracking system with a counterweight. Journal of Cleaner Production, 195, 1217-1233. [DOI: 10.1016/j.jclepro.2018.05.257]

[8] Ebrahimi, S., et al. (2019). A hybrid neural network and astronomical method for solar tracking. Energy Conversion and Management, 199, 111907. [DOI: 10.1016/j.enconman.2019.111907]

[9] Abu Mallouh, M., et al. (2019). Open-source, low-cost, solar-powered water quality monitoring system. HardwareX, 6, e00076. [DOI: 10.1016/j.ohx.2019.e00076]

[10] Karthik, K., et al. (2021). An adaptive neuro-fuzzy inference system-based maximum power point tracking controller for photovoltaic systems. International Transactions on Electrical Energy Systems, 31(2), e12734. [DOI: 10.1002/2050-7038.12734]